Geology

Zircon xenocrysts in Tibetan ultrapotassic magmas: Imaging the deep crust through time

Dong Liu, Zhidan Zhao, Di-Cheng Zhu, Yaoling Niu and T. Mark Harrison

Geology 2014;42;43-46
doi: 10.1130/G34902.1

Notes

Zircon xenocrysts in Tibetan ultrapotassic magmas: Imaging the deep crust through time

Dong Liu[1], Zhidan Zhao[1]*, Di-Cheng Zhu[1], Yaoling Niu[1,2], and T. Mark Harrison[3]
[1]State Key Laboratory of Geological Processes and Mineral Resources, and School of Earth Science and Resources, China University of Geosciences, Beijing 100083, China
[2]Department of Earth Sciences, Durham University, Durham DH1 3LE, UK
[3]Department of Earth and Space Sciences, University of California–Los Angeles, Los Angeles, California 90095-1567, USA

ABSTRACT

Zircons entrained in mantle-derived magmas offer a unique opportunity to identify cryptic magmatic episodes in the deep crust and thus to image lithospheric thickening and crustal evolution. We investigated zircon xenocrysts from mantle-derived ultrapotassic rocks in southern Tibet to evaluate their potential as a probe of crustal evolution. Similar age (Proterozoic–Paleozoic) distributions of these zircons and those in the Lhasa terrane detrital spectra demonstrate the continental origin of xenocrysts with high U/Yb. Time-progressive variations in zircon $\varepsilon_{Hf}(t)$ reveal three major magmatic pulses ca. 90, 50, and 20 Ma, suggesting significant crustal growth in the Lhasa terrane at those times. This is consistent with major mantle inputs previously documented from surface rocks in the Lhasa terrane. Increasing Dy_N/Yb_N and U/Yb since ca. 55 Ma are interpreted to reflect progressive crustal thickening in response to the India-Asia convergence. Zircon xenocrysts with varying U-Pb ages and heterogeneous Hf isotopes indicate assimilation of Lhasa terrane crust in the genesis of ultrapotassic magmas.

INTRODUCTION

Since its separation from Gondwana (Zhu et al., 2011a), the Lhasa terrane has undergone a series of subduction events that have modified the crust through successive magmatic pulses (Yin and Harrison, 2000; Chung et al., 2005; Ji et al., 2009; Zhu et al., 2011b, 2013). However, plateau uplift associated with the continued India-Asia convergence has also led to extensive erosion in southern Tibet (Harrison et al., 1992; Yin and Harrison, 2000; Hetzel et al., 2011) that may have obscured once-exposed magmatic records, and thus hampers understanding of the evolution of the Lhasa terrane.

As typical mantle-derived high-Mg rocks (MgO > 3 wt%), postcollisional ultrapotassic volcanics (UPV) in southern Tibet carry not only information on mantle sources, but also signals from crustal fragments entrained during magma ascent (Miller et al., 1999; Nomade et al., 2004; Zhao et al., 2009). These UPV rocks contain abundant zircon xenocrysts of pre-eruption age (cf. Liu et al., 2011), offering a prime opportunity to reveal signatures of magmatic pulses hidden in the deep crust of the Lhasa terrane. Using a combined in situ method of zircon chronology, trace element, and Hf isotope geochemistry, we present a systematic study of these xenocrystic zircons. Our zircon data show a more detailed pattern of mantle input, crustal reworking, and thickening in the central Lhasa subterrane than those revealed from surface rocks and, as a case study, our findings underscore the potential of zircon xenocrysts from mantle-derived magmas to image crustal evolution through time.

TECTONIC SETTING AND ULTRAPOTASSIC MAGMATISM

The Lhasa terrane, characterized by reworked ancient crust in the center and juvenile additions to both its northern and southern edges, can be subdivided into the northern, central, and southern subterranes (Zhu et al., 2011b). In the northern and central Lhasa subterranes, Early Cretaceous granitoid magmatism and coeval volcanic rocks (ca. 143–102 Ma) are widely exposed as a result of either southward subduction of the Bangong-Nujiang Tethyan seafloor (Zhu et al., 2011b, 2013) or northward flat-slab subduction of the Neo-Tethyan oceanic lithosphere (cf. Kapp et al., 2007a). The Gangdese batholith (Triassic–Cenozoic) and Linzizong volcanic rocks (ca. 63–40 Ma) distributed in the southern Lhasa subterrane are interpreted as resulting from the Neo-Tethyan oceanic seafloor subduction and subsequent India-Asia continental collision (cf. Chung et al., 2005). After the India-Asia collision in the early Paleogene, postcollisional magmatism in southern Tibet (including the Tethyan Himalaya) mainly consists of potassic-ultrapotassic volcanic rocks, adakitic intrusive rocks, and S-type granitoids (cf. Chung et al., 2005; Aikman et al., 2008; Zhao et al., 2009; Liu et al., 2011).

The majority of the Miocene UPV rocks are restricted to the central Lhasa subterrane, forming a magmatic belt roughly parallel to the east-west–trending direction of the Lhasa terrane (Fig. 1A). These UPV rocks commonly occur as bedded lava flows unconformably overlying the Cretaceous–Paleogene volcano-sedimentary strata (Miller et al., 1999; Nomade et al., 2004; Liu et al., 2011); some crop out as dikes crosscutting Cretaceous Xigaze marine forearc strata in the southern Lhasa subterrane. Crustal xenoliths are abundant in the UPV rocks (Figs. 1B–1D).

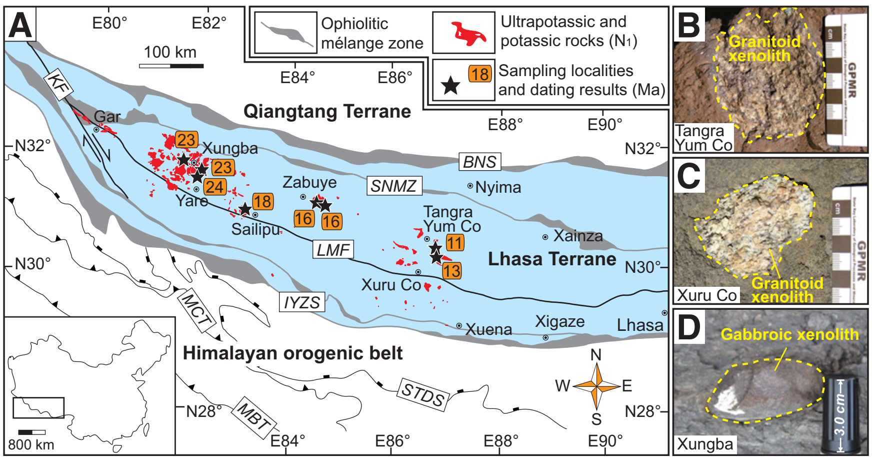

Figure 1. A: Geologic map showing sample localities and spatial distribution of postcollisional ultrapotassic-potassic rocks in southern Tibet. BNS—Bangong-Nujiang suture zone; SNMZ—Shiquan River–Nam Tso mélange zone; LMF—Luobadui-Milashan fault; KF—Karakorum fault; IYZS—Indus-Yarlung Zangbo suture zone; STDS—Southern Tibetan detachment system; MCT—Main Central thrust; MBT—Main Boundary thrust. B–D: Field photos of variety of crustal xenoliths (dashed lines) identified in Miocene ultrapotassic rocks.

*E-mail: zdzhao@cugb.edu.cn.

GEOLOGY, January 2014; v. 42; no. 1; p. 43–46; Data Repository item 2014011 | doi:10.1130/G34902.1 | Published online 22 November 2013

ANALYTICAL METHODS

The UPV rocks sampled from the central Lhasa subterrane (Fig. 1A) were crushed to 80 mesh after excluding obvious crustal xenoliths by hand-picking. Zircons extracted from such UPV host rocks were mounted in epoxy and polished to expose grain interiors. Detailed descriptions of the UPV samples, zircon cathodoluminescence images, in situ analytical methods, analytical data, and data plots are given in the GSA Data Repository[1].

RESULTS

Zircons in nine UPV samples yield U-Pb ages ranging from 3134 Ma to 10 Ma (657 analyses; Tables DR1 and DR2 and Fig. DR2 in the Data Repository) and are mostly of Mesozoic–Cenozoic age (160–10 Ma). These zircons define three major age peaks ca. 90, 50, and 20 Ma (Fig. 2A). The youngest zircon groups in each sample vary from 24 Ma in the west to 10 Ma in the east (Fig. 1A), consistent with previously published Miocene eruptive ages (Table DR1). Zircons with older U-Pb ages are xenocrystic. Except for some ca. 90 Ma zircons with homogeneous interiors, most Mesozoic–early Paleogene zircon xenocrysts show clear oscillatory zoning (Fig. DR1). In contrast, the youngest zircons (24–10 Ma) are unzoned or typically exhibit weak zoning (Fig. DR1).

The UPV zircons have a wide range of $\varepsilon_{Hf}(t)$ values (the deviation of the initial Hf isotopic ratio between the zircon sample and chondritic reservoir) that define three major perturbations at ca. 120–80 Ma, 60–45 Ma, and 25–10 Ma (Fig. 2B). In the Mesozoic population, zircon $\varepsilon_{Hf}(t)$ values yield a rapidly increasing trend (from −15.4 to +5.5) in the Early Cretaceous (ca. 120 Ma), followed by a decreasing trend (from +6.9 to −11.6) in the Late Cretaceous (ca. 80 Ma). In the Cenozoic populations, zircons are characterized by highly variable $\varepsilon_{Hf}(t)$ values (from −11.9 to +12.5) during the early Paleogene (ca. 60–45 Ma) and then by decreasing $\varepsilon_{Hf}(t)$ at ca. 45 Ma (from +5.1 to −13.5; Fig. 2B). Compared with the Mesozoic and early Paleogene zircons, zircon $\varepsilon_{Hf}(t)$ values are overall low throughout the Miocene (−21.2 to +1.2; Fig. 2B).

The Th/U of zircons in UPV rocks range from 5.1 to 0.1 (Table DR3; Fig. 3A), except for a few with Th/U < 0.07 (Fig. 3A). The UPV zircons have similar positive Ce and negative Eu anomalies (Fig. DR3). However, relative to middle rare earth elements (MREEs), their enrichments of heavy (H) REEs are different. Some zircons, with U-Pb ages younger than 55 Ma, have generally low HREE/MREE, whereas other zircons show elevated HREE abundances (Fig. DR3).

DISCUSSION

Origin of Zircon Xenocrysts in Ultrapotassic Rocks

Previous studies revealed that postcollisional UPV rocks in the Lhasa terrane have continental crust–like Sr-Nd-Pb isotopic signatures and high $\delta^{18}O$ (cf. Miller et al., 1999; Nomade et al., 2004; Zhao et al., 2009), although major element compositions are consistent with their being of mantle origin. Such contrasting features of crust- and mantle-derived magmas imply that zircon xenocrysts in UPV rocks could have originated from a metasomatized mantle reservoir or been entrained during magma ascent through the crust.

Zircons with pre-eruption ages have been identified from mantle xenoliths and mantle-derived rocks, as exemplified by the kimberlite and mantle xenoliths from the Kaapvaal craton and alkaline basalt from the Eger rift (cf. Konzett et al., 2000; Siebel et al., 2009), suggesting that pre-eruptive metasomatism in mantle sources can be recorded by mantle zircons. However, the majority of zircon xenocrysts in the Tibetan UPV rocks are not mantle derived, but instead have continental crust affinity, for the following reasons. Mantle zircons are characterized by lacking pronounced Eu anomalies, low Th and U contents (in mantle zircons from phlogopite-bearing peridotite and kimberlite), and anomalously high Th/U (>3 in zircons from veined harzburgite; Fig. 3A) (cf. Konzett et al., 2000; Hoskin and Schaltegger, 2003; Siebel et al., 2009). These are in contrast to most zircon xenocrysts in the UPV rocks that display negative Eu anomalies (Fig. DR3), high Th and U abundances, and varying but relatively low Th/U (2.5–0.07; Fig. 3A). Furthermore, the relatively high U/Yb values of UPV zircons are consistent with a continental crust origin rather than being inherited from recycled oceanic crust characterized by low U/Yb (Fig. 3B) (Grimes et al., 2007). These observations, together with the crustal xenoliths found in the UPV rocks (Figs. 1B–1D), make the Lhasa terrane and underthrust Indian continent as the two potential provenances for zircons in the UPV rocks. Given that the 160–55 Ma magmatism is very rare in the northern Indian crust (Yin and Harrison, 2000; Zhu et al., 2013) but is extensive in the Lhasa terrane (Chung et al., 2005; Wen et al., 2008; Ji et al., 2009; Zhu et

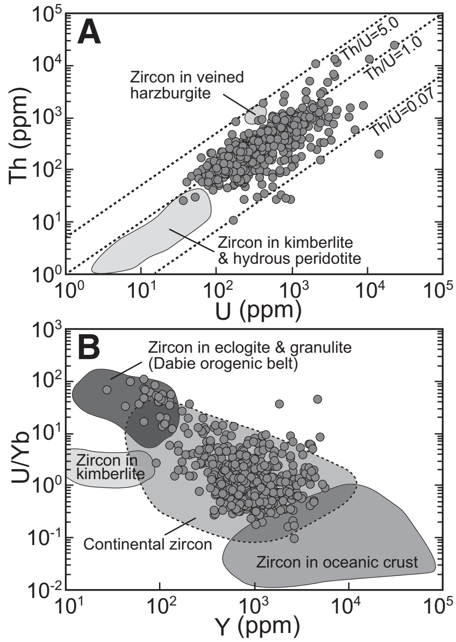

Figure 3. Discriminant diagrams for zircon origin. A: Th versus U. B: U/Yb versus Y (Grimes et al., 2007), showing crustal affinities of zircons from ultrapotassic rocks. Data of zircons in metasomatized mantle peridotites and veined harzburgite are from Konzett et al. (2000, and references therein). Fields of zircons in eclogite and granulite from Dabie orogenic belt are shown for comparison (cf. Wang et al., 2012).

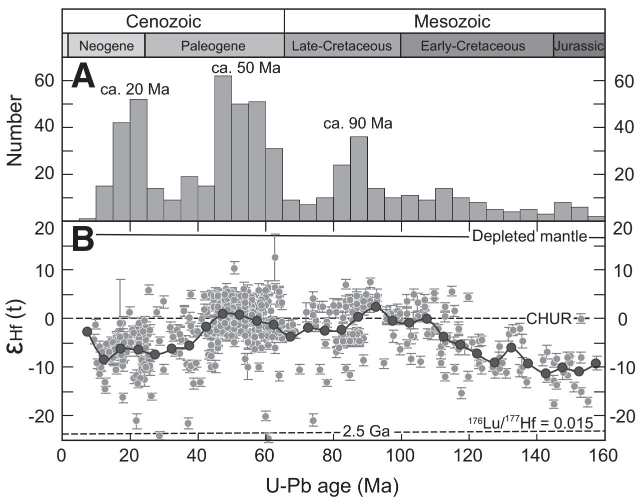

Figure 2. A: Histogram of U-Pb ages for zircons in ultrapotassic rocks. Three major magma stages can be identified at ca. 90, 50, and 20 Ma. B: Time-correlated variations defined by zircon $\varepsilon_{Hf}(t)$ values of zircon xenocrysts (ca. 160 Ma or later). Only concordant zircon data are used. Black circles are average $\varepsilon_{Hf}(t)$ values in 5 m.y. time windows. Details of the data, chondritic uniform reservoir (CHUR) line, and dashed parallel lines of Hf crustal model ages (T_{DM}^{C}) are given in Tables DR2 and DR4 (see footnote 1).

[1]GSA Data Repository item 2014011, detailed analytical methods, sample description, in-situ analytical data (Tables DR1–DR4), and Figures DR1–DR4, is available online at www.geosociety.org/pubs/ft2014.htm, or on request from editing@geosociety.org or Documents Secretary, GSA, P.O. Box 9140, Boulder, CO 80301, USA.

al., 2011b), we conclude that the Lhasa terrane crust is the dominant provenance for zircon xenocrysts in the UPV rocks, and assimilation of Lhasa crust plays a significant role in the petrogenesis of the Tibetan ultrapotassic rocks.

Zircon Records of Crustal Reworking During Mesozoic–Cenozoic Magmatism

Crustal formation and reworking processes are thought to be closely related to magmatism and its associated thermal perturbation during plate convergence (Hawkesworth and Kemp, 2006). Substantial mantle input into magma can be recorded by zircon Hf isotopic ratios because the emplacement of voluminous basaltic magmas will enable more primitive magmas to crystallize zircons with high $\varepsilon_{Hf}(t)$ values. Zircons preserved in the UPV rocks reveal three magmatic pulses in the deep crust, all of which are marked by varying Hf isotopic compositions (Fig. 2). Based on the continental crust origin, we interpreted such magmatic pulses presented by UPV zircons as indicating significant mantle inputs that can be linked to the crustal formation and reworking in the central Lhasa subterrane at those times.

The interpretation here is further supported by the correspondence between UPV zircon records and surface rocks related to the crustal growth in the Lhasa terrane (Wen et al., 2008; Ji et al., 2009; Zhu et al., 2011b, 2013). The Mesozoic crustal growth recorded by UPV zircon Hf isotopes commenced at ca. 115 Ma with an increasing trend in $\varepsilon_{Hf}(t)$ that remains high until ca. 90 Ma (Fig. 2B), possibly corresponding to the 113 ± 5 Ma magmatic flare-up postulated to result from slab break-off of the southward-subducting Bangong-Nujiang Tethyan seafloor (Zhu et al., 2011b, 2013) and/or the rollback of the Neo-Tethyan subducting slab (ca. 100–80 Ma; cf. Wen et al., 2008). The relatively high $\varepsilon_{Hf}(t)$ values of the early Paleogene (ca. 60–45 Ma) zircons (Fig. 2B) are similar to the syncollisional magmatic records in the southern Lhasa subterrane (cf. Ji et al., 2009; Zhu et al., 2013), which can be explained by rollback and subsequent break-off of the Neo-Tethyan oceanic slab (ca. 65–45 Ma; Chung et al., 2005; Ji et al., 2009) and/or by Asian plate lithospheric removal (ca. 69–50 Ma; Kapp et al., 2007b). The wide range of Miocene zircon $\varepsilon_{Hf}(t)$ values (>10 ε units) suggests a continued mantle contribution to the postcollisional magmatism, which could have been triggered by convective thinning of overthickened lithospheric mantle (Chung et al., 2005; Zhao et al., 2009; Liu et al., 2011) or rollback of subducted Indian lithosphere (Nomade et al., 2004).

Crustal Thickening History Recorded in Zircon Xenocrysts

Some UPV zircon xenocrysts have extremely high U/Yb ratios and low HREE/MREE ratios (Fig. DR3), similar to those in zircons of eclogite and granulite origin (Fig. 3B). Given the increasing enrichment of HREEs displayed by zircons from adakitic rocks ($Dy_N/Yb_N < 0.3$; Guan et al., 2012), the nearly flat HREE patterns in UPV zircons are not observed in any well-documented crustal suite and cannot have crystallized from the highly HREE-depleted adakitic magmas because of zircons' strong preference for HREEs (Rubatto, 2002; Hoskin and Schaltegger, 2003). We interpret such HREE-depleted zircons with relatively high Th/U ratios (94% of analyses > 0.2) and concordant U-Pb ages as having crystallized under a very limited HREE supply.

One possible source supplying very limited HREEs is the melting residues after adakite melt extraction deep in the lower crust under eclogite facies conditions. With the presence of abundant garnet in such melting residues, the incompletely extracted interstitial residual melt would be expected to be highly depleted in HREEs. Zircons crystallized from such residual melt would therefore have low HREEs. This scenario suggests that the adakitic magmatism would occur earlier than ultrapotassic magmatism, and can be supported from the field observation that postcollisional volcanism in the Xungba area consists of ultrapotassic rocks and underlying coeval potassic rocks with adakitic geochemical signatures (Liu et al., 2011). Thus, we suggest that zircons with high Dy_N/Yb_N and U/Yb are indicative of thickened crust with eclogite and garnet-bearing granulitic lower crust. In this regard, the systematic changes in UPV zircon trace elements, i.e., that the Dy_N/Yb_N and U/Yb ratios remain low until ca. 55 Ma and then rise dramatically (Fig. 4), can be interpreted as the consequence of significant crustal thickening of the central Lhasa subterrane at that time. Such interpretation in terms of zircon geochemical data is corroborated by Eocene adakitic rocks in the Gangdese batholith (51–38 Ma; Guan et al., 2012; Ji et al., 2012), high Sr/Y granitoids in the Tethyan Himalaya (ca. 44 Ma; Aikman et al., 2008), and the results of thermochronological studies (cf. Hetzel et al., 2011), all of which suggest a complicated crustal shortening history initiated before or in the early stage of the India-Asia continental collision (Kapp et al., 2007b; Hetzel et al., 2011).

A notable feature of Figure 4 is that no distinct excursions of Dy_N/Yb_N and U/Yb ratios are seen in the Mesozoic zircon xenocrysts; this is different from Cenozoic zircons. This implies that crustal thickening in the central Lhasa subterrane did not reach the threshold beyond which HREE depletion in zircons was triggered.

Implications for Postcollisional Ultrapotassic Magmatism

The Tibetan Miocene ultrapotassic magmas are generally thought to represent melts of enriched mantle sources, and to be capable of tracing subduction events (cf. Miller et al., 1999; Zhao et al., 2009). However, the presence of abundant zircon xenocrysts and a wide range of zircon $\varepsilon_{Hf}(t)$ values observed in the Miocene UPV zircons (25–10 Ma) indicate that materials across the full range of the lithosphere may have contributed to the UPV magmas. At least two kinds of crustal component may have been involved: juvenile lower crust and ancient Lhasa basement (middle-upper crust). Input from juvenile lower crust that might have been overthickened during India-Asia convergence can be supported by the entrained gabbroic xenoliths (Fig. 1D) and the positive $\varepsilon_{Hf}(t)$ values of ca. 90 and 50 Ma zircon xenocrysts in the UPV rocks (Fig. 2B). Contribution from ancient Lhasa basement is supported by the presence of Proterozoic and Paleozoic zircon xenocrysts, the age distributions (two age peaks ca. 450 Ma and ca. 1050 Ma) and Hf isotopic compositions of which are comparable to the detrital zircon spectra in Permian–Carboniferous metasedimentary strata (Zhu et al., 2011a) and inherited zircons in S-type granite (ca. 206 Ma; Zhu et al., 2011a, 2013) from the Lhasa terrane (Fig. 5).

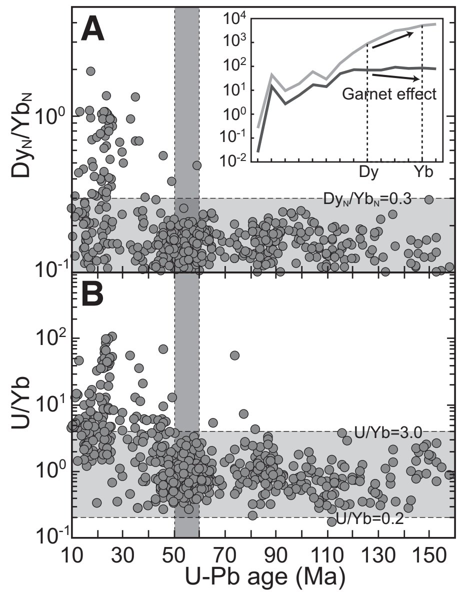

Figure 4. Time-progressive variations of zircon Dy_N/Yb_N and U/Yb ratios, showing that crustal thickening may have begun at ca. 55 Ma in response to the India-Asia collision.

CONCLUSIONS

Continental-like signatures in the UPV zircons indicate a xenocrystic origin during magma ascent through the deep crust, corroborating the role of crustal contaminants in the petrogenesis of the UPV host rocks. These zircon xenocrysts yield $\varepsilon_{Hf}(t)$ values and U-Pb ages indicative of three major magmatic pulses ca. 90, 50, and 20 Ma that correlate well with both crustal reworking and thickening histories of southern Tibet and match well with the known magmatic

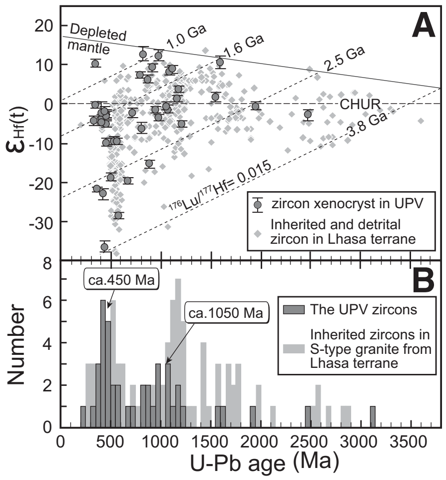

Figure 5. A: Plot of $\varepsilon_{Hf}(t)$ versus U-Pb age. B: U-Pb age histogram, showing Hf isotopic compositions and age distribution of Paleozoic–Proterozoic zircon xenocrysts in ultrapotassic rocks (UPV). ^{206}Pb/^{238}U and ^{207}Pb/^{206}Pb ages are used for zircons younger than 1000 Ma and older than 1000 Ma, respectively. The $\varepsilon_{Hf}(t)$ values of inherited zircons and detrital zircon records of Lhasa terrane are plotted for comparison (Zhu et al., 2011a). U-Pb age distribution of inherited zircons from Triassic S-type granite (ca. 206 Ma) shows similar age distribution between UPV zircon records and those from central Lhasa subterrane.

history of the Lhasa terrane. Distinctive geochemical signatures of zircon xenocrysts since ca. 55 Ma are best interpreted as reflecting significant crustal thickening in response to ongoing India-Asia convergence.

ACKNOWLEDGMENTS

We thank Paul Kapp and two anonymous reviewers for constructive critical reviews. We thank Yongsheng Liu and Zhaochu Hu for guidance in analyses of zircon U-Pb, Lu-Hf isotopes, and trace elements. This study was supported by the China 973 Program (projects 2011CB403102, 2009CB421002), the National Science Foundation of China (grants 41273044, 41225006), the U.S. National Science Foundation (grants EAR-1111959, EAR-1111586), Sinoprobe-04-02, IRT1083, and the China Ministry of Education 111 Program (B07011).

REFERENCES CITED

Aikman, A.B., Harrison, T.M., and Lin, D., 2008, Evidence for early (>44 Ma) Himalayan crustal thickening, Tethyan Himalaya, southeastern Tibet: Earth and Planetary Science Letters, v. 274, p. 14–23, doi:10.1016/j.epsl.2008.06.038.

Chung, S.L., Chu, M.F., Zhang, Y., Xie, Y., Lo, C.H., Lee, T.Y., Lan, C.Y., Li, X., Zhang, Q., and Wang, Y., 2005, Tibetan tectonic evolution inferred from spatial and temporal variations in post-collisional magmatism: Earth-Science Reviews, v. 68, p. 173–196, doi:10.1016/j.earscirev.2004.05.001.

Grimes, C.B., John, B.E., Kelemen, P.B., Mazdab, F.K., Wooden, J.L., Cheadle, M.J., Hanghøj, K., and Schwartz, J.J., 2007, Trace element chemistry of zircons from oceanic crust: A method for distinguishing detrital zircon provenance: Geology, v. 35, p. 643–646, doi:10.1130/G23603A.1.

Guan, Q., Zhu, D.C., Zhao, Z.D., Dong, G.C., Zhang, L.L., Li, X.W., Liu, M., Mo, X.X., Liu, Y.S., and Yuan, H.L., 2012, Crustal thickening prior to 38 Ma in southern Tibet: Evidence from lower crust-derived adakitic magmatism in the Gangdese Batholith: Gondwana Research, v. 21, p. 88–99, doi:10.1016/j.gr.2011.07.004.

Harrison, T.M., Copeland, P., Kidd, W.S.F., and Yin, A., 1992, Raising Tibet: Science, v. 255, p. 1663–1670, doi:10.1126/science.255.5052.1663.

Hawkesworth, C.J., and Kemp, A.I.S., 2006, Evolution of the continental crust: Nature, v. 443, p. 811–817, doi:10.1038/nature05191.

Hetzel, R., Dunkl, I., Haider, V., Strobl, M., von Eynatten, H., Ding, L., and Frei, D., 2011, Peneplain formation in southern Tibet predates the India-Asia collision and plateau uplift: Geology, v. 39, p. 983–986, doi:10.1130/G32069.1.

Hoskin, P.W.O., and Schaltegger, U., 2003, The composition of zircon and igneous and metamorphic petrogenesis: Reviews in Mineralogy and Geochemistry, v. 53, p. 27–62, doi:10.2113/0530027.

Ji, W.Q., Wu, F.Y., Chung, S.L., Li, J.X., and Liu, C.Z., 2009, Zircon U-Pb geochronology and Hf isotopic constraints on petrogenesis of the Gangdese batholith, southern Tibet: Chemical Geology, v. 262, p. 229–245, doi:10.1016/j.chemgeo.2009.01.020.

Ji, W.Q., Wu, F.Y., Liu, C.Z., and Chung, S.L., 2012, Early Eocene crustal thickening in southern Tibet: New age and geochemical constraints from the Gangdese batholith: Journal of Asian Earth Sciences, v. 53, p. 82–95, doi:10.1016/j.jseaes.2011.08.020.

Kapp, P., DeCelles, P.G., Gehrels, G.E., Heizler, M., and Ding, L., 2007a, Geological records of the Lhasa-Qiangtang and Indo-Asian collisions in the Nima area of central Tibet: Geological Society of America Bulletin, v. 119, p. 917–933, doi:10.1130/B26033.1.

Kapp, P., DeCelles, P.G., Leier, A., Fabijanic, J.M., He, S., Pullen, A., Gehrels, G.E., and Ding, L., 2007b, The Gangdese retroarc thrust belt revealed: GSA Today, v. 17, no. 7, p. 4–9, doi:10.1130/GSAT01707A.1.

Konzett, J., Armstrong, R.A., and Günther, D., 2000, Modal metasomatism in the Kaapvaal craton lithosphere: Constraints on timing and genesis from U-Pb zircon dating of metasomatized peridotites and MARID-type xenoliths: Contributions to Mineralogy and Petrology, v. 139, p. 704–719, doi:10.1007/s004100000160.

Liu, D., Zhao, Z.D., Zhu, D.C., Wang, Q., Sui, Q.L., Liu, Y.S., Hu, Z.C., and Mo, X.X., 2011, The petrogenesis of post-collisional potassic-ultrapotassic rocks in Xungba basin, western Lhasa terrane: Constraints from zircon U-Pb geochronology and geochemistry: Acta Petrologica Sinica, v. 27, p. 2045–2059.

Miller, C., Schuster, R., Kltzli, U., Frank, W., and Purtscheller, F., 1999, Post-collisional potassic and ultrapotassic magmatism in SW Tibet: Geochemical and Sr-Nd-Pb-O isotopic constraints for mantle source characteristics and petrogenesis: Journal of Petrology, v. 40, p. 1399–1424, doi:10.1093/petroj/40.9.1399.

Nomade, S., Renne, P.R., Mo, X., Zhao, Z., and Zhou, S., 2004, Miocene volcanism in the Lhasa block, Tibet: Spatial trends and geodynamic implications: Earth and Planetary Science Letters, v. 221, p. 227–243, doi:10.1016/S0012-821X(04)00072-X.

Rubatto, D., 2002, Zircon trace element geochemistry: Partitioning with garnet and the link between U-Pb ages and metamorphism: Chemical Geology, v. 184, p. 123–138, doi:10.1016/S0009-2541(01)00355-2.

Siebel, W., Schmitt, A.K., Danišík, M., Chen, F., Meier, S., Weiß, S., and Eroğlu, S., 2009, Prolonged mantle residence of zircon xenocrysts from the western Eger rift: Nature Geoscience, v. 2, p. 886–890, doi:10.1038/ngeo695.

Wang, S.J., Li, S.G., An, S.C., and Hou, Z.H., 2012, A granulite record of multistage metamorphism and REE behavior in the Dabie orogen: Constraints from zircon and rock-forming minerals: Lithos, v. 136, p. 109–125, doi:10.1016/j.lithos.2011.11.001.

Wen, D.R., Liu, D.Y., Chung, S.L., Chu, M.F., Ji, J.Q., Zhang, Q., Song, B., Lee, T.Y., Yeh, M.W., and Lo, C.H., 2008, Zircon SHRIMP U-Pb ages of the Gangdese Batholith and implications for Neotethyan subduction in southern Tibet: Chemical Geology, v. 252, p. 191–201, doi:10.1016/j.chemgeo.2008.03.003.

Yin, A., and Harrison, T.M., 2000, Geologic evolution of the Himalayan-Tibetan orogen: Annual Review of Earth and Planetary Sciences, v. 28, p. 211–280, doi:10.1146/annurev.earth.28.1.211.

Zhao, Z., Mo, X., Dilek, Y., Niu, Y., DePaolo, D.J., Robinson, P., Zhu, D., Sun, C., Dong, G., and Zhou, S., 2009, Geochemical and Sr-Nd-Pb-O isotopic compositions of the post-collisional ultrapotassic magmatism in SW Tibet: Petrogenesis and implications for India intra-continental subduction beneath southern Tibet: Lithos, v. 113, p. 190–212, doi:10.1016/j.lithos.2009.02.004.

Zhu, D.C., Zhao, Z.D., Niu, Y., Dilek, Y., and Mo, X.X., 2011a, Lhasa terrane in southern Tibet came from Australia: Geology, v. 39, p. 727–730, doi:10.1130/G31895.1.

Zhu, D.C., Zhao, Z.D., Niu, Y., Mo, X.X., Chung, S.L., Hou, Z.Q., Wang, L.Q., and Wu, F.Y., 2011b, The Lhasa terrane: Record of a microcontinent and its histories of drift and growth: Earth and Planetary Science Letters, v. 301, p. 241–255, doi:10.1016/j.epsl.2010.11.005.

Zhu, D.C., Zhao, Z.D., Niu, Y., Dilek, Y., Hou, Z.Q., and Mo, X.X., 2013, Origin and pre-Cenozoic evolution of the Tibetan Plateau: Gondwana Research, v. 23, p. 1429–1454, doi:10.1016/j.gr.2012.02.002.

Manuscript received 3 July 2013
Revised manuscript received 11 September 2013
Manuscript accepted 2 October 2013

Printed in USA